

## Comparative Study of Selective Laser Melting and Direct Laser Metal Deposition of Ni<sub>3</sub>Al Intermetallic Alloy

**D. Kotoban<sup>1</sup>, A. Nazarov<sup>1</sup>, and I. Shishkovsky<sup>1,2</sup>**

<sup>1</sup> Moscow State University of  
Technology “STANKIN”,  
Vadkovsky pereulok 3a, 127055  
Moscow, Russia

<sup>2</sup> Lebedev Physics Institute (LPI) of  
Russian Academy of Sciences,  
Samara branch, Novo-Sadovaja st.  
221, 443011 Samara, Russia  
kotobandv@mail.ru

Selective laser melting (SLM) and Direct laser metal deposition (DLMD) are well known additive manufacturing processes to produce complex net-shaped and nearly net-shaped parts. Both methods provide significant freedom in the design of metal parts, which leads to an increase in the performance of metal components. This study involves SLM and DLMD to produce 3D-objects to obtain apparent comparative data [1]. Taking in account the economics of additive manufacturing, the methods of SLM and DMLD could be precisely attracted to aerospace, energy and automotive industries. Against this background, an intermetallic alloy of nickel aluminides Ni<sub>3</sub>Al was used as a promising material. Intermetallic  $\gamma$  and  $(\gamma + \gamma')$  Ni<sub>3</sub>Al phases have melting point of about 1385 °C, low density ( $\sim 7.53 \text{ g/cm}^3$ ), thermal stability up to melting, increase in the yield point up to 900 °C, and a high heat resistance up to 1250 °C [2–5]. A nickel aluminide powder H85IO15 (JSC “Polema”, Russia) was used in this study with the stoichiometric composition of Ni<sub>3</sub>Al phase. The powder fraction was +20 -63  $\mu\text{m}$ .

The experiments were carried out on the DLMD machine equipped with Yb:YAG disc laser of 2kW maximum output power with a wavelength of 1.03  $\mu\text{m}$ . An experimental facility (designed and developed in MSTU “STANKIN”) was used to investigate SLM-process. The facility consists of an ytterbium fiber laser source LK-200-B (IPG-Photonics, Russia) with 200 W maximum output power in about 100  $\mu\text{m}$  laser beam diameter (with wavelength of 1.07  $\mu\text{m}$ ), an optical focusing system based on beam expander, a galvanometer

optical scanner, an F-Theta lens, and a powder bed with a mechanism for depositing and leveling off the powder and for moving the manufacturing platform.

To characterize the microstructures, the specimen was cross-cut, grinded and polished. For the optical microscopy (Olympus BX51, Japan) certain specimens were exposed to etching in acetic acid:  $\text{HNO}_3$  : HCl solution in volume ratio 10:10:15 to investigate the structure. A hardness testing was carried out on microhardness tester PMT-3M (Russia) and Qness Q10A (Austria). Surface morphology and enhanced studying of microstructures and defects were carried out with a TESCAN VEGA 3 LMH scanning electron microscope (Czech Rep.) equipped with an energy-dispersive X-ray analyzer.

For the SLM, the laser power and the beam scanning speed were used as variables. The powder layer thickness was constant (70  $\mu\text{m}$ ). The beam diameter on the surface was 100  $\mu\text{m}$ . The laser scanning speed was 10–20 mm/min, and the laser power varied within a range of 40–200 W. The hatching distance was about the beam diameter, and the layer depth was 70  $\mu\text{m}$ .

For the DLMD, three parameters were used as variables: the laser power was 80–500 W, the scanning speed was 50–600 mm/min, and the powder feed rate was 3.8–9.0 g/min. The laser beam diameter was 200  $\mu\text{m}$ , and the process was carried out at the optical and powder focal point. The hatching distance was 150  $\mu\text{m}$ , and the layer depth was 150-200  $\mu\text{m}$ .

Both processes show the manufacturability of the nickel aluminide material used. For single-track experiments, we obtained a number of tracks with a variety of cross-section geometry. There was no general dissimilarity in the track geometry except unsteady process parameters. The side view of the tracks with appropriate process parameters was continuous and uniform; this was interpreted as a good outcome for layering processing. No cracks or pores were revealed for both processes.

After the preliminary study of hatching distances, one-layer specimens and multilayer 3D objects were manufactured. The

obtained specimens show smooth layered side-view structure typical of additive manufacturing. The initial dimensions of the multilayered specimens (cubes) were 7x7x5 mm, and the measured dimensions for SLM and DLMD specimens were 7.2x7.2x5 mm and 7.4x7.4x5 mm (averaged), respectively. The predicted error is due to the fact that the dimension points of the model are at the center of laser beam but the specimen dimensions are above by a beam radius on the side. The measured dimensions error is higher for two reasons: a mechanical system error and overheating of the ends of tracks, which could lead to melting of more powder.

The microstructures were similar for both processes and show columnar dendritic structures with main dendrite arms about 15–20  $\mu\text{m}$ , secondary dendrite arms about 5–8  $\mu\text{m}$ , and grain size about 45  $\mu\text{m}$  (Fig. 1). The fine structure of the specimens is related to the process parameters and directly to the laser treatment, which leads to high-speed cooling. The element analysis shows a uniform distribution of nickel and aluminum in aspect ratio close to the stoichiometric ratio of  $\text{Ni}_3\text{Al}$ .

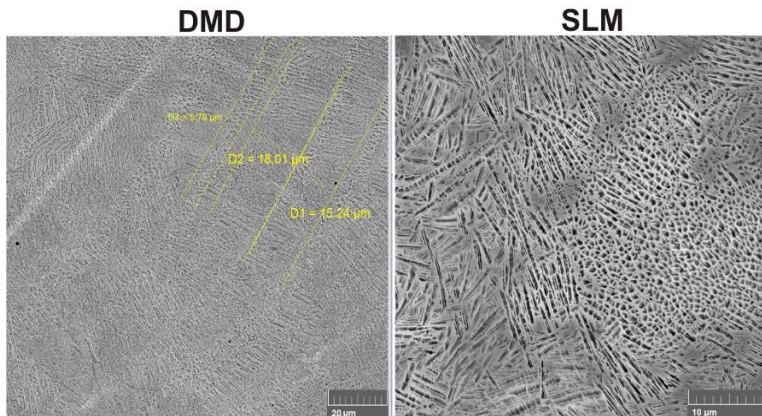


Figure 1: SEM image of DLMD and SLM microstructures. Parameters for DLMD: laser power = 500W, scanning speed = 600 mm/min, powder feed = 3.8 g/min. Parameters for SLM: laser power = 150W, scanning speed = 720 mm/min.

The multilayered specimens show cracks that develop in the bulk and propagate through the layers. Under lower scanning speed, fewer cracks were observed. The crack initiation was in the cooling stages with reference to the microstructures.

A phase-structural analysis shows similar results for both SLM and DLMD specimens. The strongest lines were obtained at angles of 51.4 and 52.1 degrees with respect to the Ni<sub>3</sub>Al phase. The attached metastable Ni<sub>2</sub>Al and ferrum trace were also identified. We point out that the crystal orientation of the  $\gamma'$ -Ni<sub>3</sub>Al has preferred direction [111].

It was concluded that there is no significant difference between SLM and DLMD in microstructure. The greater laser beam of DLMD leads to a different dimension error, but in fact, the DLMD is worse in reproducing the contours of 3D-models with worse surface conditions. This imperfection of DLMD is compensated for by more flexibility and by the faster technological cycle.

The authors would like to thank the support of Russian Science Foundation (grant agreement 14-19-00992).

## References

- [1] *I. V. Shishkovsky*, Laser controlled intermetallics synthesis during surface cladding, pp. 237–286. J. Lawrence et.al. (Eds.), Laser Surface Engineering. Processes and applications, Woodhead Publishing Series in Electronic and Optical Materials, Elsevier Science & Technology, on-line ISBN 978-1-78242-074-3. 2015. 718 p.
- [2] *B. A. Grinberg and M. A. Ivanov*. Intermetallidy Ni<sub>3</sub>Al and TiAl: Microstructure and Deformation Behavior. UrO RAN, Yekaterinburg, 2002. 360p.
- [3] *S. Zhu et. al.* Ni<sub>3</sub>Al matrix high temperature self-lubricating composites. Tribology International. Vol. 44. No. 4, pp. 445–453. 2011.
- [4] *W. Liu and J. N. DuPont*. Direct laser deposition of a single-crystal Ni<sub>3</sub>Al-based IC221W alloy. Metallurgical and Materials Transactions A. Vol. 36. No. 12, pp. 3397–3406. 2005.